The Triassic-Liassic volcanic sequence and rift evolution in the Saharan Atlas basins (Algeria). Eastward vanishing of the Central Atlantic magmatic province

A. Meddah, H. Bertrand, A. Seddiki, M. Tabeliouna

Geologica Acta, Vol.15, Nº 1, March 2017, 11-23, I
DOI: 10.1344/GeologicaActa2017.15.1.2

geologica acta

The Triassic-Liassic volcanic sequence and rift evolution in the Saharan Atlas basins (Algeria). Eastward vanishing of the Central Atlantic magmatic province

A. MEDDAH[1] H. BERTRAND[2*] A. SEDDIKI[3] M. TABELIOUNA[3]

[1]Centre Universitaire de Tindouf, Laboratoire GEOREN
Tindouf, 37000, Algérie

[2]Laboratoire de Géologie de Lyon, Terre, Planètes, Environnement, UMR 5276 CNRS, Observatoire de Lyon, Université et Ecole Normale Supérieure de Lyon
46 allée d'Italie, 69364 Lyon Cedex 07, France. Bertrand e-mail: herve.bertrand@ens-lyon.fr

[3]Faculté des Sciences de la Terre et de l'Univers, Laboratoire GEOREN, Université d'Oran
BP.1015, El Mnaouer, Oran, 31000, Algérie

*Corresponding author

ABSTRACT

We investigate the Triassic-Liassic sequence in ten diapirs from the Saharan Atlas (Algeria). Based on detailed mapping, two episodes are identified. The first one consists of a volcano-sedimentary sequence in which three volcanic units were identified (lower, intermediate and upper units). They are interlayered and sometimes imbricated with siliciclastic to evaporitic levels which record syn-sedimentary tectonics. This sequence was deposited in a lagoonal-continental environment and is assigned to the Triassic magmatic rifting stage. The second episode, lacking lava flows (post magmatic rifting stage), consists of carbonate levels deposited in a lagoonal to marine environment during the Rhaetian-Hettangian. The volcanic units consist of several thin basaltic flows, each 0.5 to 1m thick, with a total thickness of 10–15m. The basalts are low-Ti continental tholeiites, displaying enrichment in large ion lithophile elements and light rare earth elements [(La/Yb)n= 2.5-6] with a negative Nb anomaly. Upwards decrease of light-rare-earth-elements enrichment (*e.g.* La/Yb) is modelled through increasing melting rate of a spinel-bearing lherzolite source from the lower (6–10wt.%) to the upper (15–20wt.%) unit. The lava flows from the Saharan Atlas share the same geochemical characteristics and evolution as those from the Moroccan Atlas assigned to the Central Atlantic magmatic province. They represent the easternmost witness of this large igneous province so far known.

KEYWORDS | **Saharan Atlas. Algeria. Volcano-evaporitic sequence. Partial melting. Central Atlantic Magmatic Province (CAMP).**

INTRODUCTION

The Central Atlantic Magmatic Province (CAMP) covers an area of ca.10^7km^2, spanning four continents: North and South America, Western Europe and Northwest Africa (Marzoli *et al.*, 1999). This magmatic event consists of large tholeiitic basalts represented by dike swarms, sills, and lava flows (Fig. 1A). It occurred at the end of the Triassic (≈200Ma) during the early stages of the Pangea rifting that led to the opening of the central Atlantic ocean

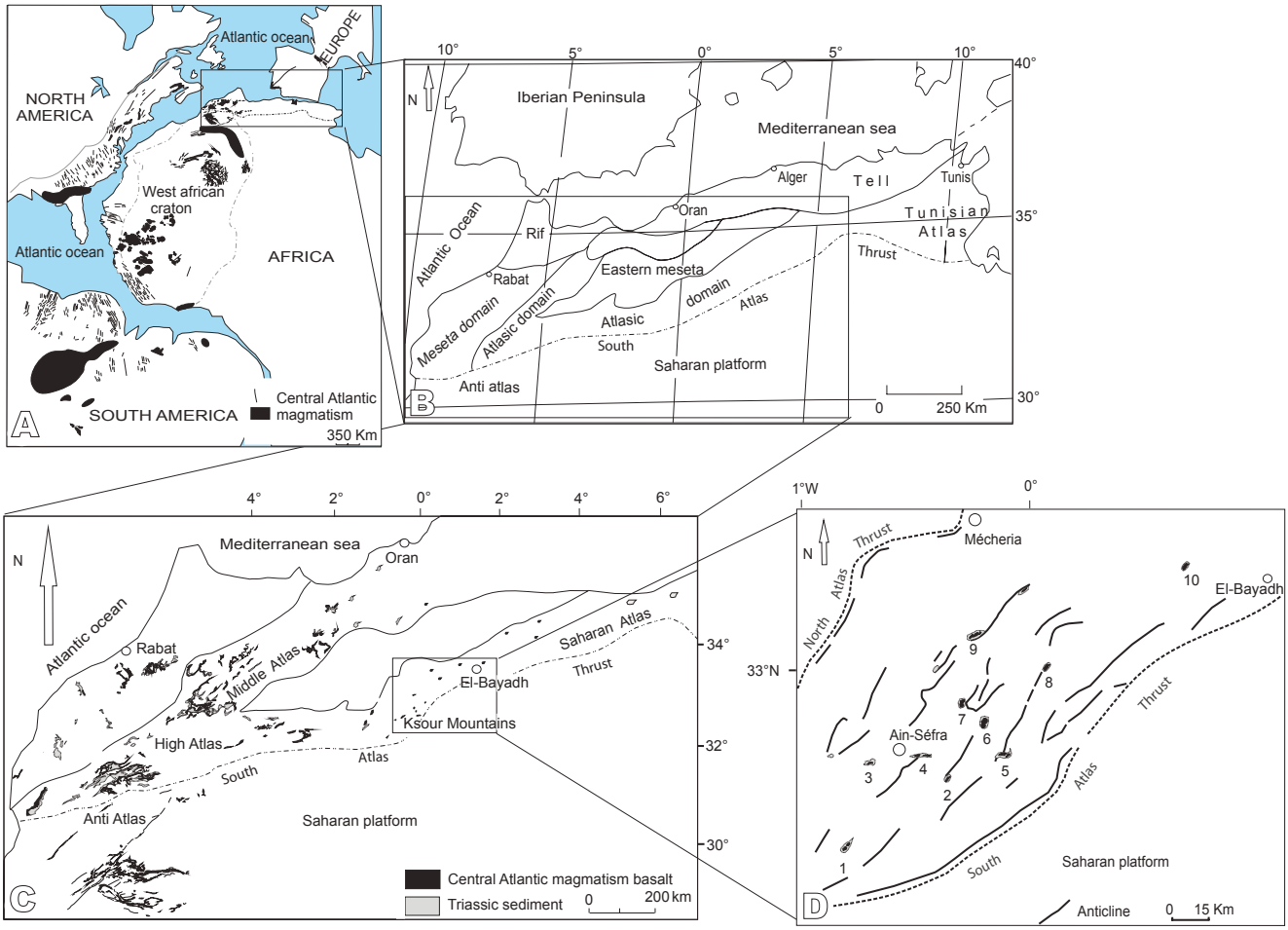

FIGURE 1. A) Schematic map of the Central Atlantic magmatic province (after Bertrand, 1991; Marzoli *et al.*, 1999; McHone, 2000; Verati *et al.*, 2005; Chabou *et al.*, 2007; Meddah *et al.*, 2007; Bertrand *et al.*, 2014); B) main geological domains of North Africa, C) distribution of CAMP volcanism in the northwest Africa with location of studied area (after Meddah *et al.*, 2007; Meddah, 2010); D) structural outline of the western Saharan Atlas, with location of the investigated Triassic diapirs (numbers 1 to 10; cf. lithological sections in Figure 3).

(Nomade *et al.*, 2007; Jourdan *et al.*, 2009; Schoene *et al.*, 2010; Marzoli *et al.*, 2011). The huge eruptions of the CAMP are likely to have triggered the Triassic-Jurassic mass extinction (Tanner *et al.*, 2004).

In Algeria, CAMP remnants outcrop in the Triassic evaporitic diapirs of the Saharan Atlas and in the Saharan Platform (Fig. 1A, B, C; Chabou *et al.*, 2007; Meddah *et al.*, 2007, Chabou *et al.*, 2010; Meddah, 2010). In Morocco, they are disseminated in the High, Middle and Anti-Atlas and in the Meseta domains (Fig. 1B, C; Bertrand *et al.*, 1982; Knight *et al.*, 2004; Marzoli *et al.*, 2004; Mahmoudi and Bertrand, 2007; Bensalah *et al.*, 2011; Farki *et al.*, 2014). In the Saharan Atlas, High and Middle Atlas and in the Meseta, the CAMP volcanic pile generally caps Triassic sedimentary series filling extensional basins (Laville and Petit, 1984; Aït Ouali, 1991; Aït Ouali and Delfaud, 1995; Piqué and Laville, 1995; Le Roy and Piqué, 2001; Yelles-Chaouche *et al.*, 2001).

The aim of this paper is: i) to present the Triassic-early Liassic volcano-sedimentary sequence in the Saharan Atlas (Algeria); ii) to compare the geochemical characteristics of the basaltic rocks from the Saharan Atlas with those from the Moroccan Atlas; iii) to constrain the geodynamic evolution of the Atlasic basins during the early Mesozoic; iv) to assess the extent of the Central Atlantic magmatic province in Algeria, in connection with the rift evolution at the end of the Triassic.

GEOLOGICAL SETTING

The Cenozoic Maghrebian orogenic domain comprises the Tell and the Rif (Maghrebides) and the Atlasic domain (Durand-Delga and Fonboté, 1980). The Tell-Rif is interpreted as an Alpine orogen resulting from the closure of the Maghrebian Tethys (Bouillin, 1986).

The Atlasic domain (Fig. 1B) is regarded as an intra-continental orogen (Mattauer *et al.*, 1977) developed on former mesozoic half-grabens initiated during the Triassic-Liassic rifting (Aït Ouali and Delfaud, 1995; Piqué and Laville, 1996; Piqué *et al.*, 1998; Frizon de Lamotte *et al.*, 2000). It is the result of strike-slip movements and reactivation of late-hercynian fractures (Mattauer *et al.*, 1977; Piqué and Laville, 1996; Piqué *et al.*, 1998). Clastic and evaporitic sequences were deposited in these half-grabens accompanied by tholeiitic basaltic flows (Aït Ouali and Delfaud, 1995; Piqué *et al.*, 1998).

In the Saharan Atlas, this volcanic episode occurred during the late Triassic (Flamand, 1911; Bassoulet, 1973; Meddah *et al.*, 2007; Meddah, 2010) and corresponds to the magmatic rifting stage, coeval with the onset of basin opening (Fig. 2). The environment was lagoonal-continental (Busson, 1974). The basaltic flows are associated with the evaporitic sediments of the Triassic diapirs. These outcrops are controlled by NE-SW anticlines (Galmier, 1970) distributed over an area of 40.000km^2.

This first episode of opening was followed by an episode of carbonate sedimentation without magmatism, corresponding to the post-magmatic rifting stage and assigned to the lower-middle Lias (Aït Ouali and Delfaud, 1995; Yelles-Chaouche *et al.*, 2001, Meddah *et al.*, 2007). This second episode is part of the carbonate platform, set

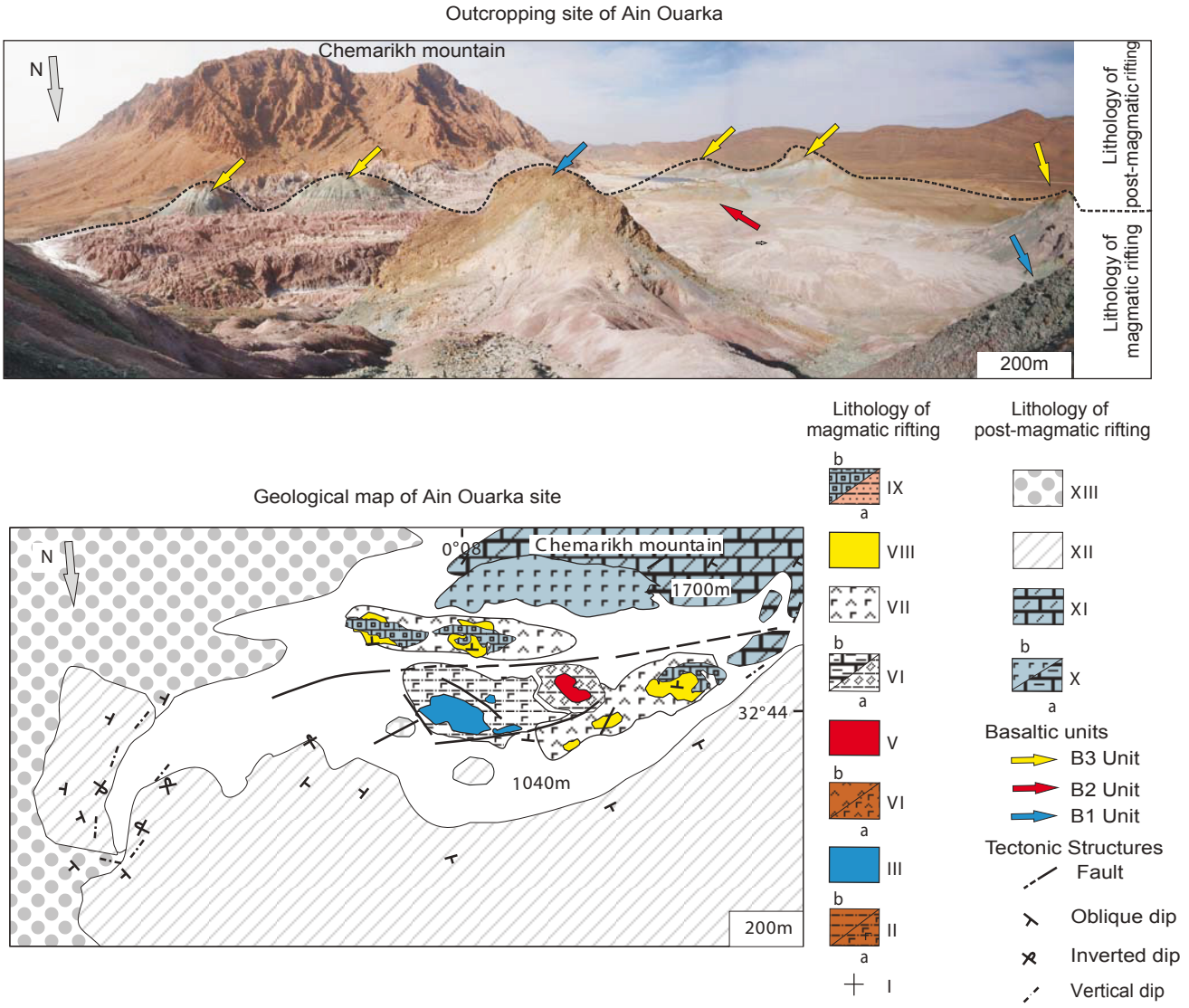

FIGURE 2. A) Example of diapiric site, showing the three volcanic units. B) Geological map of Ain Ouarka site, I) substratum; IIa) saliferous clay; IIb) red claystone with hematite; III) unit B1; IVa) red saliferous clay; IVb) red gypsiferous clay; V) volcanic unit B2; VIa) carbonated clay; VIb) argillaceous limestone with laminar stromatolitic structure; VII) gypsiferous and saliferous marls; VIII) volcanic unit B3; IXa) red carbonated clay; IXb) black clay-siliceous limestone with laminar stromatolitic structure; Xa) limestone with laminar stromatolitic structure; Xb) saliferous marls; XI) dolomite (Hettangian); XII) limestone marl (undifferentiated Jurassic); XIII) conglomerate (Tertiary).

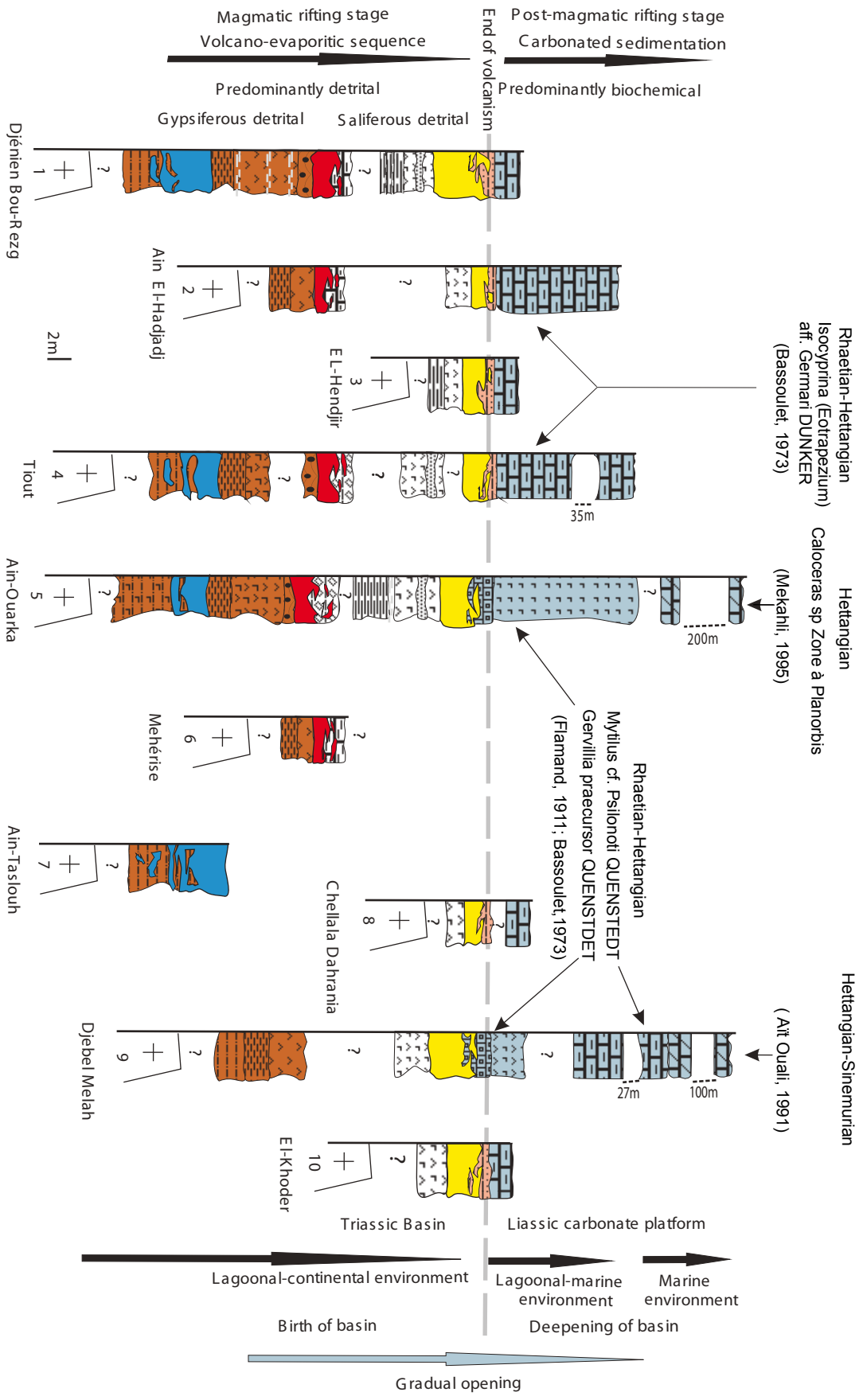

FIGURE 3. Stratigraphic sections (location of sites in Figure 1D; same legend as in Figure 2).

up during the early deepening of the basin (Fig. 3) in a lagoonal-marine to marine environment (Flamand, 1911; Aït Ouali and Delfaud, 1995; Piqué *et al.*, 1998; Yelles-Chaouche *et al.*, 2001). This episode ended during the Domerian and was followed by the upper Lias post-rift filling of the basin (Aït Ouali and Delfaud, 1995; Yelles-Chaouche *et al.*, 2001).

STRATIGRAPHIC SECTIONS

Based on detailed mapping of the diapiric sites (*e.g.* Fig. 2), 10 stratigraphic sections are reported in Figure 3. Inter-sites correlations allow to establish a lithological sequence subdivided into two groups. The lower group consists of Triassic volcano-evaporitic deposits corresponding to the magmatic rift stage. The upper group consists of Rhaetian-Hettangian limestones corresponding to the post-magmatic rift stage. At the eastern end of the Saharan Atlas, beyond the longitude 5ºE, the diapiric sites are constituted by undifferentiated whitish saliferous marls, lacking magmatic or carbonate material.

Magmatic rift stage

The lower group is characterized by three volcanic units interlayered with a siliciclastic-evaporitic sequence (Figs. 2; 3): the lower volcanic unit B1 (5 to 7m thick), the intermediate volcanic unit B2 (1.5 to 3.5m thick) and the upper volcanic unit B3 (4 to 6m thick). Each volcanic unit consists of several thin basaltic flows, 0.5 to 1m thick. Individual lava flows show a massive aspect at the base and evolve towards a vesicular upper crust (Fig. 4). The vesicles are millimeter-sized and rounded. In the massive part of the flows, the basaltic rocks have well-preserved magmatic textures and mineralogy. Most basaltic lavas display a fine to medium-grained aphanitic structure, except the Djénien Bou-Rezg basalts from the lower unit which contain millimeter-sized grains of olivine phenocrysts. Dominant textures are intergranular to subophitic (Fig. 5A, D, E), sometimes with a glomeroporphyritic tendency in the lava flows of unit B2 (Fig. 5C). The petrography of the volcanic units is relatively homogeneous. Mineral assemblages are composed by partially resorbed olivine, Ca-plagioclase, clinopyroxene (augite) and minor amounts of titanomagnetite (Fig. 5A, E). A granophyric interstitial phase has been observed in the B1 lava flows from Tiout (Fig. 5B). This primary mineral assemblage is typical of the continental tholeiites forming the CAMP province, particularly in Morocco (*e.g.* Bertrand, 1991). As a whole, the basalts from the Saharan Atlas are more altered than those from Morocco (Meddah *et al.*, 2007). The main alteration phases include mica-type (after plagioclase), epidote and calcite (after pyroxene) and iddingsite-chlorite (after olivine).

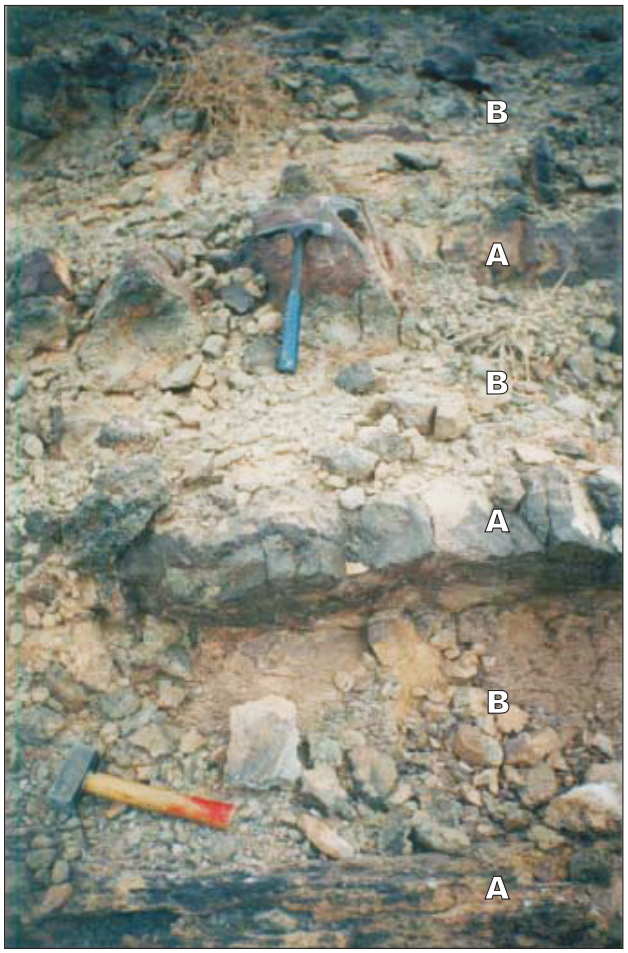

FIGURE 4. Example of volcanic flows (Unit B1, Djenien Bou-Rezg site). A) Massive aspect at the base. B) Vesicular upper part.

The sedimentary sequence evolves from detrital gypsiferous lithologies below the B2 basaltic unit to detrital saliferous lithologies upwards. Mingling relationships are observed between sedimentary and volcanic materials at the base of B1 and at the top of B2 and B3 lava units (Figs. 3; 6). In Ain-Ouarka area, the B1 lava flows penetrate hematite-bearing, locally saliferous, red claystones, resulting in a mixture of both lithologies (Fig. 6). The B2 lavas penetrate argillaceous limestones (1.5m thick) displaying laminar stromatolitic structure in Djénien Bou-Rezg, Ain-El-Hadjadj and Méhérise areas and penetrate carbonated clay (3.5 to 4m thick) in Tiout and Ain-Ouarka areas (Fig. 6). The B3 lavas penetrate red carbonated clay (0.2 to 0.3m thick) in Djénien Bou-Rezg, Ain-El-Hadjadj, El-Hendjir, Tiout and Chellala Dahrania areas. In Ain-Ouarka and Djebel Melah areas, these same lava flows penetrate black clay-siliceous limestone with laminar stromatolitic structure (Fig. 6). This latter facies has 1.5 to 2.5m thick and contains the bivalve *Gervillia praecursor* Quenstedt (Flamand, 1911; Bassoulet, 1973).

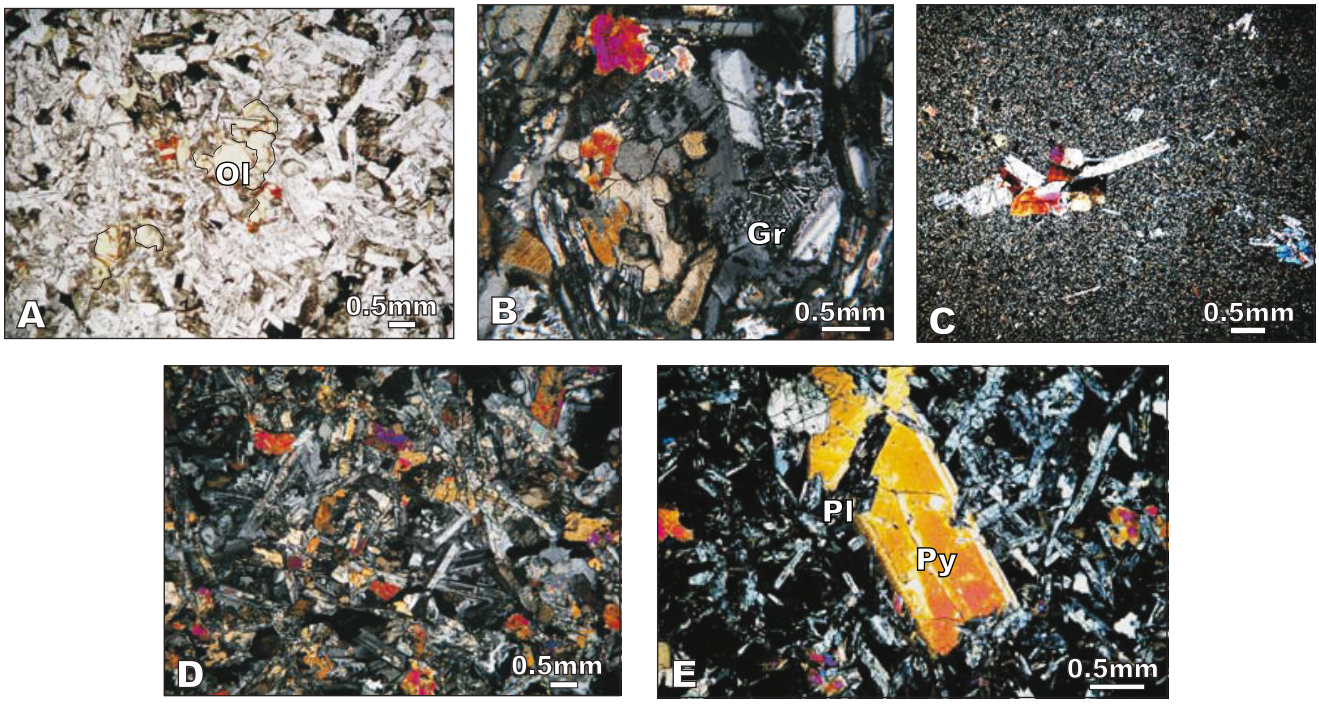

FIGURE 5. Microscopic views. A) Intergranular texture with olivine (Unit B1); B) Section showing granophyric phase (Unit B1); C) Glomeroporphyric texture (Unit B2); D) Intergranular texture (Unit B3); E) Subophitic texture (Unit B3). (Pl: plagioclase; Py: pyroxene; Ol: olivine; Gr: granophyric phase). A) Plane polarized light; B, C, D and E) crossed polarized light.

Syn-sedimentary tectonics has been observed in layers associated with the volcanic flows of the various units. The tectonics is ductile in the argillaceous limestone with laminar stromatolitic levels associated with the B2 lava flows (Fig. 7A), whereas it is more brittle in the black clay-siliceous limestone with laminar stromatolitic levels associated with the B3 lava flows and in the limestones which top the volcano-evaporitic sequence. In the latter two cases, the disruption of sedimentary layers, with reverse fault, is characterized by the formation of monogenic breccias (Fig.7B, B', C).

Post-magmatic rift stage

As it is the case in the whole Atlasic area (Aït Ouali, 1991; Aït Ouali and Delfaud, 1995; Piqué *et al.*, 1998), carbonate sedimentation predominates after volcanism ceases all over the study area except in Ain-Ouarka and Djebel Melah where saliferous marls are deposited (Figs. 2; 3). Carbonate deposits consist of finely bedded limestones with laminar stromatolitic structure, dolomites and marls. They contain the bivalve *Isocyprina* (*Eotrapezium*) aff. *germari* (Dunker) assigned to Rhaetian-Hettangian (Bassoulet, 1973). In Ain-Ouarka, saliferous marls are overlain by the Djebel Chémarikh dolomite containing the ammonite Caloceras sp. Planorbis zone (Mékahli, 1995), whereas in Djebel Melah, they are overlain by limestones with the bivalve *Mytilus* cf. *psilonoti* Quenstedt (Flamand, 1911; Bassoulet, 1973). The latter limestones are overlain by the Hettangian-Sinemurian dolomite (Aït Ouali, 1991; Aït Ouali and Delfaud, 1995). These paleontological data are consistent with the late Triassic age assigned to the magmatic rift stage.

GEOCHEMISTRY

Analytical methods

The analyzed samples represent 9 areas (8 areas from the western part and one area from the central part of the Saharan Atlas). 34 samples (12 from the unit B1, 5 from the unit B2 and 17 from the unit B3) have been analyzed for major and trace elements (Cr, Ni, Co, Sc, V and Y) using X-ray fluorescence (XRF spectrometer Phillips PW 1404) at the Earth Science Laboratory, University of Lyon. H_2O^- and H_2O^+ are loss on ignition measured at 100ºC and 1100ºC, respectively. The precision is 1 to 2wt.% for major elements and 10 to 15wt.% for trace elements. Rare earth elements (REE) and Rb, Sr, Zr, Nb, Ba, Hf, Th, U and Ta were analyzed using Inductively Coupled Plasma Mass Spectrometry (ICP-MS) at the Ecole Normale Supérieure de Lyon on eight samples from the three lava units, selected among the least altered. Rock powder (200mg) was dissolved in a mixture of 3ml

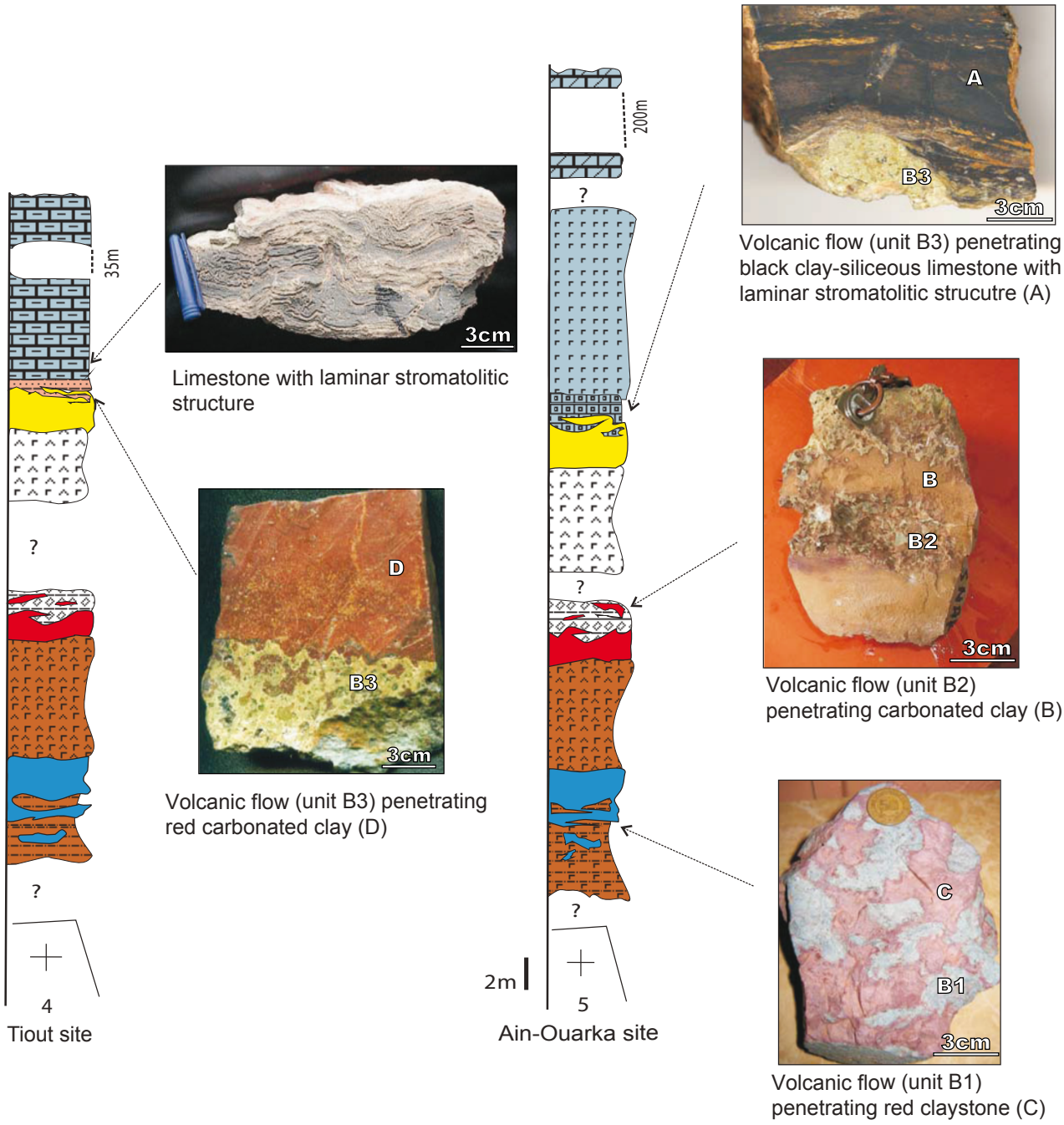

FIGURE 6. Macroscopic characteristics of the lithologies associated with the volcanic flows. Same legend as in Figure 2.

HF and 1ml HNO_3 during 48h on a hot plate (130°C) under a 50bars pressure. The solutions were evaporated, dried and the residues dissolved in 25ml HNO_3 (0.5N). These solutions were diluted to 0.1ml and analyzed with a VG Element plasma quadripole II ICP-MS with electron multiplier. The precision is 3 to 15wt.% according to each of the elements. The standard used for all analyses was BHVO-1.The major and trace element compositions are listed in Table I, Appendix I.

Major and trace element composition

Loss On Ignition (LOI) ranges from 1.27 to 4.31wt.%, which indicates significant alteration, in agreement with the petrographic observations. The alteration process was likely responsible for a post-magmatic increase in the amount of total alkalis (*e.g.* K_2O varies between 1.3 and 4.65wt.% with an extreme value at 7.16wt.%; Na_2O varies from 0.35 to 3.5wt.%). The rocks are therefore shifted

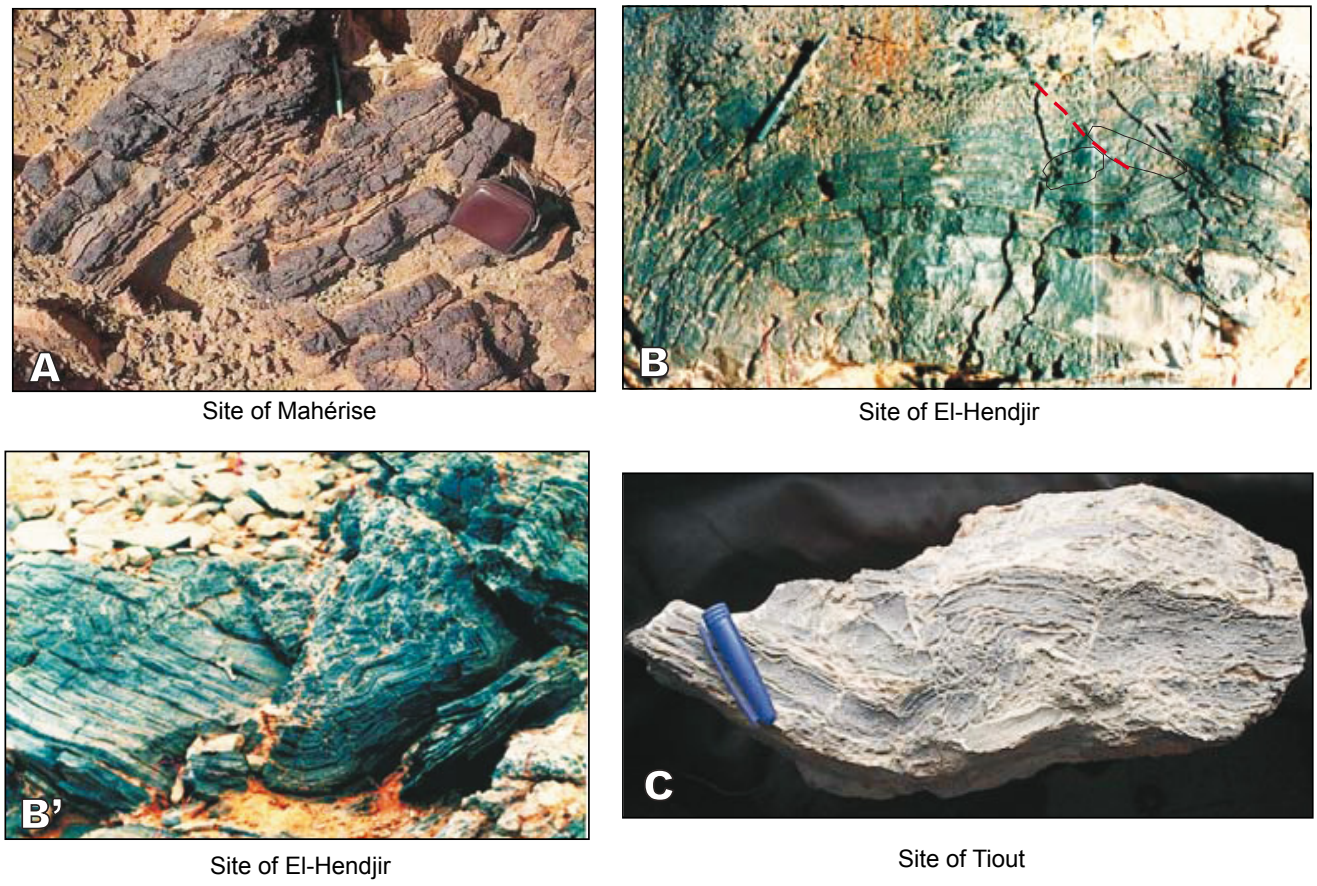

FIGURE 7. Syn-sedimentary tectonics. A) Argillaceous limestone showing ductile tectonics; B, B') Black clay-siliceous limestone with the laminar stromatolitic structure showing the disruption of sedimentary layers with reverse fault; formation of monogenic breccia in the stratification plane (B) and in the fold axis (B'); C) Limestone with laminar stromatolitic structure (same observations as in B and B').

out of the CAMP field in the total alkalis *versus* silica classification plot (Le bas *et al.*, 1986; Fig. 8A). However, based on less mobile elements such as Ti, Zr, Nb, Y (Floyd and Winchester, 1975; Winchester and Floyd, 1977), the rocks closely match other CAMP basalts such as those of the lava flows in the Moroccan Atlas (Fig. 8B, C). They are classified as subalkaline basalts and andesitic basalts (Fig. 8B) and continental tholeiites (Fig. 8C). All are low-Ti tholeiites, with TiO_2 contents ranging from 1.02wt.% to 1.58wt.%, and low P_2O_5 (0.10–0.20wt.%) and Zr (95–161ppm) contents. The TiO_2 content decreases from the lower to the upper unit (Table I). The rocks are moderately differentiated with Mg-numbers [Mg#] ranging between 0.53 and 0.64.

Chondrite-normalized Rare Earth Elements (REE) patterns (Fig. 9A) exhibit a negative slope, with significant enrichment in Light Rare Earth Elements (LREE) compared to the Heavy REE (HREE). Notably, the LREE enrichment decreases from the lower ([La/Yb]n~6) to intermediate ([La/Yb]n~4) and to the upper ([La/Yb]n~2.5) units. In the Mid-Ocean Ridge Basalt (MORB) normalized multi-element spider diagram (Fig. 9B), the studied samples display a strong enrichment in Large Ion Lithophile Elements (LILE) compared with High Field Strength Elements (HFSE), with a distinct negative anomaly in Nb. The variability of Ba and Rb is likely due to alteration processes.

DISCUSSION

Basalts in the Saharan Atlas: the easternmost witness of the CAMP

Basalts in the Saharan Atlas are low-Ti continental tholeiites which match the chemical compositions of other CAMP lava flows, especially those from the Moroccan Atlas (Marzoli *et al.*, 2004; Mahmoudi and Bertrand, 2007), based on major and trace elements the least sensitive to alteration processes (Fig. 8B). Notably, the three lava units identified here show the same chemical evolution as the three major units from Morocco. This evolution is characterized by a decreasing LREE/HREE (*e.g.* La/Yb) ratio from the base towards the top of the

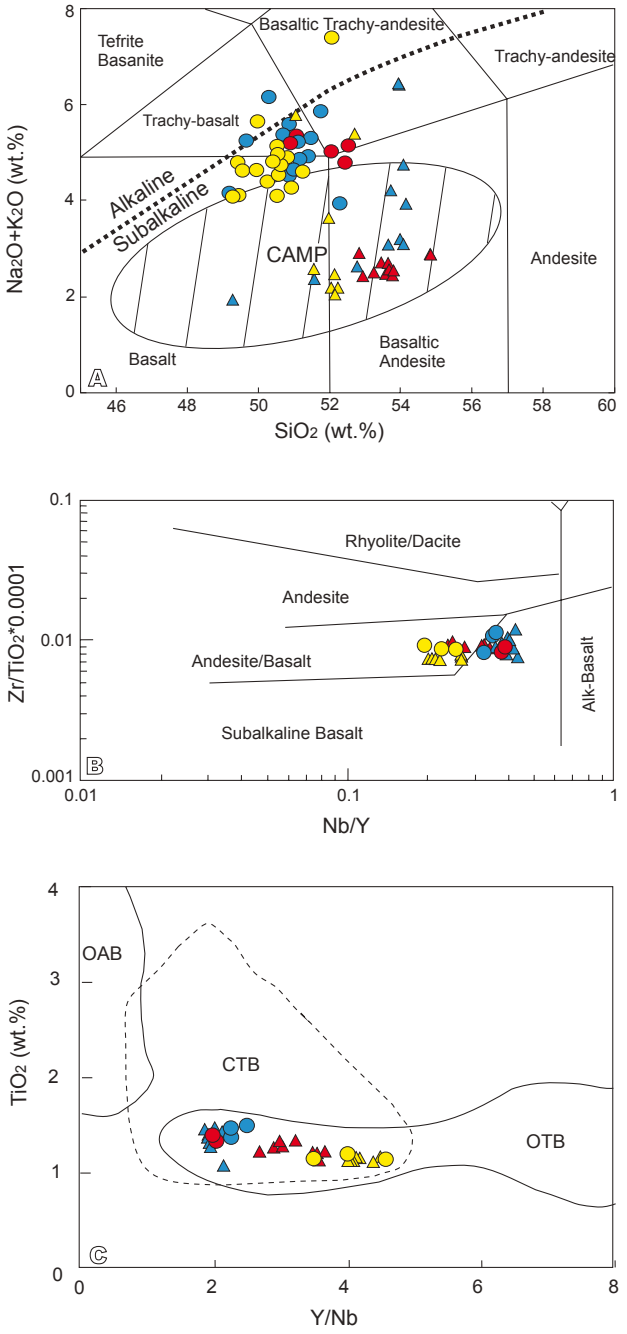

FIGURE 8. A) Total Alkali-Silica diagram (Le Bas et al., 1986) for volcanic rocks from the Saharan Atlas. Data for CAMP domain after McHone (2000); B) Diagram of (Zr/TiO_2)*0.0001 *versus* Nb/Y (Winchester and Floyd, 1977) for volcanic rocks from the Saharan Atlas; C) Discrimination diagram TiO_2 versus Y/Nb (Floyd and Winchester, 1975) for volcanic rocks of the Saharan Atlas. OAB: Oceanic Alkali Basalts; CTB: Continental Tholeiitic Basalts; OTB: Oceanic Tholeiitic Basalts. Blue symbols: lower unit; red symbols: intermediate unit; yellow symbols: upper unit; circles: Saharan Atlas; triangles: Moroccan Atlas (from Marzoli *et al.*, 2004; Mahmoudi and Bertrand, 2007).

lava pile (Fig. 9A), suggesting that similar magma sources and processes were operating in both regions. Upward fractionation of La/Yb for a constant Dy/Yb ratio argues for partial melting occurring in the spinel stability field and precludes the involvement of garnet in the mantle source, as discussed by Thirlwall *et al.* (1994) and Bogaard and Worner (2003). The data are best reproduced by a model of batch partial melting of a spinel lherzolite, which would require increasing degrees of partial melting from approximately 6-10wt.% for the lower unit to 10–15wt.% for the intermediate unit and 15–20wt.% for the upper unit (Fig. 10). In the absence of isotope data, further assessment of the mantle sources is beyond the scope of this paper (see discussions in Callegaro *et al.*, 2014; Merle *et al.*, 2014).

The volcanic sequence in the Saharan Atlas differs from the Moroccan one in two points: i) the younger, so-called recurrent, lava unit observed in the Moroccan High Atlas (Bertrand *et al.*, 1982; Marzoli *et al.*, 2004) is lacking in the Saharan Atlas; ii) the thickness of the lava sequence is considerably reduced from west (up to 300m in the Moroccan High Atlas, ibid.) to east (10–15m in the Saharan Atlas, Fig. 2). No lava flows remnants are observed beyond 5ºE. The volcanic sequence in the Saharan Atlas is therefore the easternmost witness of the CAMP recorded to date in northwest Africa, 1000km away from the Moroccan high Atlas. It represents the vanishing activity of this large igneous province.

CAMP volcanism and rift evolution in the Saharan Atlas

In northwest Africa, the formation of small Triassic-Liassic intracontinental basins was controlled by the reactivation of older Hercynian structures during rifting events at the onset of the dislocation of the Pangea (Laville and Petit, 1984; Laville and Piqué, 1991; Piqué and Laville, 1995, 1996; Piqué *et al.*, 1998). In the Saharan Atlas, small basins were initiated by tilted block faulting during the Upper Triassic (Rhaetian), as attested by geophysical studies (Kazi-Tani, 1986; Yelles-Chaouche, 2001; Belfar, 2004).

In the study area, the CAMP volcanism punctuates the early development of these rift basins (Fig. 11). The three lava units were outpouring in a lagoonal-continental environment, closely linked and sometimes imbricated with evaporitic deposits, forming the volcano-evaporitic sequence of rifting. As the rifting progresses, the degree of melting increases from 6–10wt.% for the lower lava unit up to 15–20wt.% for the upper lava unit.

Syn-sedimentary tectonics is attested by the disruption of the sedimentary beds associated with the volcanic units, resulting in the formation of monogenic breccias. These structures are similar to those described in the Briançonnais zone (French

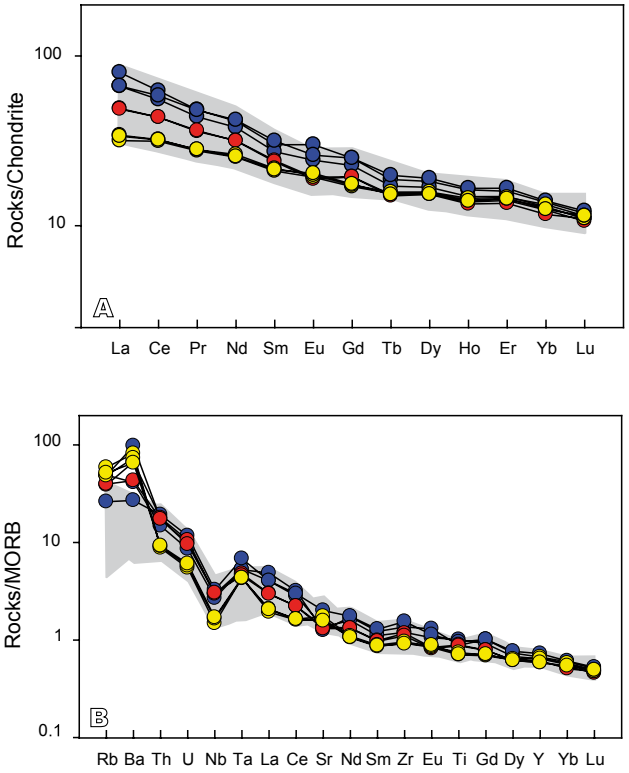

FIGURE 9. A) REE patterns of the basaltic rocks from the Saharan Atlas normalized to chondrites (Sun and McDonough, 1989); B) MORB normalized multi-element patterns for volcanic rocks from the Saharan Atlas (normalization values are from Hofmann, 1988). Same symbols and same data source for Morocco as in Figure 8. Moroccan field in grey.

western Alps), which indicate the instability of the substratum and Triassic block tilting (formation of half-grabens) in a distensive context (Megard-Galli and Faure, 1988).

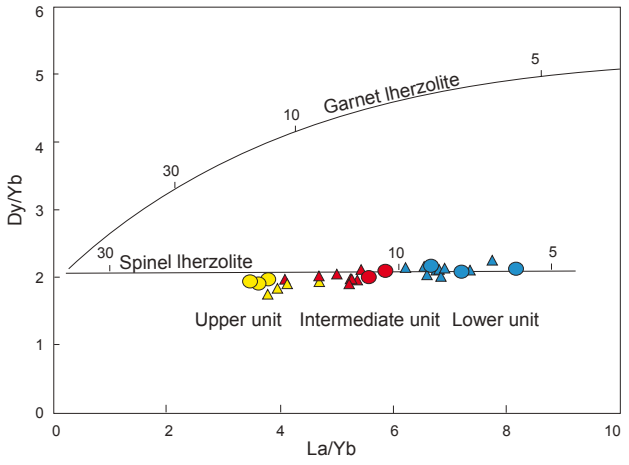

FIGURE 10. Dy/Yb *versus* La/Yb diagram for volcanic rocks from the Saharan Atlas and the Moroccan Atlas. The models of batch partial melting of spinel lherzolite and garnet lherzolite sources are from Thirlwall *et al.*, 1994. Ticks on the curves indicate degrees of melting. Same symbols and same data source for Morocco as in Figure 8.

The cessation of the volcanic activity coincides with the transition from a dominantly evaporitic sedimentation (synmagmatic-rift stage) to the progressive marine incursion resulting in the development of the Liassic carbonate platform (postmagmatic-rift stage).

CONCLUSIONS

i) The three basaltic lava-flow units from the Triassic-Liassic basins of the Saharan Atlas share the same stratigraphic position (Upper Triassic) and the same chemical composition as those from the CAMP in Morocco. As such, they are part of the CAMP volcanism.

ii) CAMP volcanism in the Saharan Atlas differs from its Moroccan counterpart because of widely lower volumes of lavas emitted. The thickness of the lava pile is 10-15m, compared to ca. 300m in the Moroccan high Atlas, 1000km away. Hence the Saharan Atlas basins host the easternmost witnesses of CAMP volcanism recognized until now which represent the vanishing activity of the CAMP. No CAMP remnant was recorded so far beyond 5ºE.

iii) CAMP lava flows from the three units are closely associated and imbricated with Triassic sedimentary levels which display syn-sedimentary tectonic features indicative of an extensional paleo-stress field.

iv) Modelling the upwards decrease of LREE enrichment suggests increasing melting rates of a spinel-bearing lherzolite, from 6–10wt.% for the lower unit up to 15–20wt.% for the upper unit. This evolution accommodates the ongoing rifting which ultimately led to the disruption of the Pangea and opening of the central Atlantic ocean.

ACKNOWLEDGMENTS

This work was supported by the ministry of higher education and scientific research of Algeria. Chantal Douchet and Paul Capiez are acknowledged for their analytical assistance. An anonymous reviewer and the Section Editor of Geologica Acta are acknowledged for their helpful comments.

REFERENCES

Aït Ouali, R., 1991. Le rifting des Monts des Ksour (Algérie occidentale) au Lias: Organisation du bassin, diagénèse des assises carbonatées. Place dans les ouvertures mésozoïques au Maghreb. Thèse Doctorat d'Etat. Algérie, Université d'Alger, 297pp.

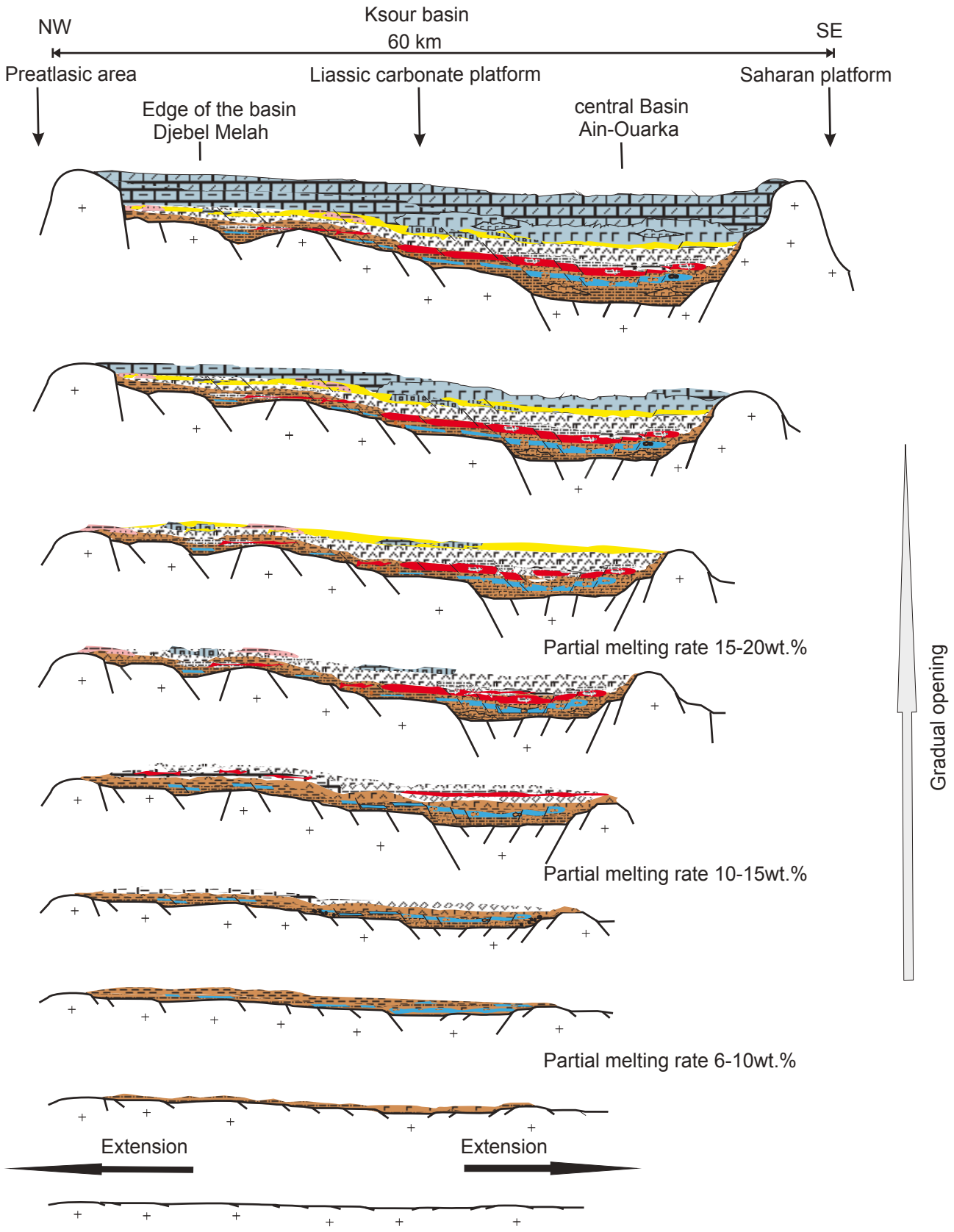

FIGURE 11. Sketch of the geodynamic evolution of the Ksour Basin (Western Saharan Atlas), during the Triassic-Lias. Legend as in Figure 2.

Aït Ouali, R., Delfaud, J., 1995. The opening procedure of Ksour basin in Lias through Jurassic rifting in the Maghreb. Comptes Rendus de l'Académie des Sciences, 320, série IIa, 773-778.

Bassoulet, J.P., 1973. Contribution à l'étude stratigraphique du Mésozoïque de l'Atlas saharien occidental (Algérie). Thèse Doctorat d'Etat. France, Université Paris 6, 497pp.

Belfar, F., 2004. Géométrie et dynamique des bassins triasiques de l'Atlas saharien occidental et des hauts plateaux (Algérie). Séminaire Géologie Pétrolière 5. Boumerdès Algérie, 150pp.

Bensalah, M.K., Youbi, N., Mahmoudi, A., Bertrand, H., Mata, J., El Hachimi, H., Madeira, J., Martins, L., Marzoli, A., Bellon, H., Medina, F., Karroum, M., Karroum, L.A., Ben Abbou, M., 2011. The Central Atlantic magmatic province (CAMP) volcanic sequences of Berrechid and Doukkala basins (Western Meseta, Morocco). Volcanology and geochemistry. Comunicações Geológicas, 98, 15-27.

Bertrand, H., 1991. The Mesozoic tholeiitic province of northwest Africa: a volcano-tectonic record of the early opening of Central Atlantic. In: Kampunzu, A.B., Lubala, R.T. (eds.). Magmatism in Extensional Structural Settings, the Phanerozoic African Plate. Springer-Verlag, 147-191.

Bertrand, H., Dostal, J., Dupuy, C., 1982. Geochemistry of early Mesozoic tholeiites from Morocco. Earth and Planetary Science Letters, 58(2), 225-239.

Bertrand, H., Fornari, M., Marzoli, A., García-Duarte, R., Sempere, T., 2014. The Central Atlantic magmatic province extends into Bolivia. Lithos, 188, 33-43.

Bogaard, P.J.F., Worner, G., 2003. Petrogenesis of basanitic to tholeiitic volcanic rocks from the Miocene Vogelsberg, Central Germany. Journal of Petrology, 44(3), 569-602.

Bouillin, J.P., 1986. Le bassin maghrébin: une ancienne limite entre l'Europe et l'Afrique à l'ouest des Alpes. Bulletin de la Société Géologique de France, 8(4), 547-558.

Busson, G., 1974. Le Trias évaporitique d'Afrique du Nord et d'Europe occidentale, données sur la paléogéographie et les conditions de dépôt. Bulletin de la Société Géologique de France, 7(XVI), 6, 653-665.

Callegaro, S., Rapaille, C., Marzoli, A., Bertrand, H., Chiaradia, M., Reisberg, L., Bellieni, G., Martins, L., Madeira, J., Mata, J., Youbi, N., DeMin, A., Azevedo, M.R., Bensalah, M.K., 2014. Enriched mantle source for the Central Atlantic magmatic province: New supporting evidence from southwestern Europe. Lithos, 188, 15-32.

Chabou, M.C., Sebai, A., Féraud, G., Bertrand, H., 2007. 40Ar/39Ar dating of the Central Atlantic magmatic province (CAMP) in southwestern Algeria. Comptes Rendus Geoscience, 339, 970-978.

Chabou, M.C., Bertrand, H., Sebai A., 2010. Geochemistry of the Central Atlantic magmatic province (CAMP) in south western Algeria. Journal of African Earth Sciences, 58, 211-219.

Durand-Delga, M., Fonboté, J.M., 1980. Le cadre structural de la Méditerranée occidentale. In: Aubouin, J., Debelmas, J., Latreille, M. (eds.). Géologie des chaînes alpines issues de la Téthys. Colloque nº5, 26º Congrès géologique international, Paris, Mémoire Bureau de Recherches Géologiques et Minières, 115, 67-85.

Farki, K., Zahour, G., El Hadi, H., Alikouss, S., Zerhouni, Y., 2014. Les tholéiites fini triasiques de Mohammedia (meseta côtière, Maroc): témoins d'un volcanisme de rift intracontinental avorté. European Scientific Journal Edition, 10(20), 125-143.

Flamand, G.B.M., 1911. Recherches géologiques et géographiques sur le Haut pays de l'Oranie et sur le Sahara (Algérie et territoire du sud). Thèse Doctorat d'Etat. Université de Lyon (France), 1001pp.

Floyd, P.A., Winchester, J.A., 1975. Magma type and tectonic setting, discrimination using immobile elements. Earth and Planetary Science Letters, 27, 211-218.

Frizon de Lamotte, D., Saint Bezar, B., Bracène, R., Mercier, E., 2000. The two main steps of the Atlas building and geodynamics of the western Mediterranean. Tectonics, 19(4), 740-761.

Galmier, D., 1970. Photogéologie de la région d'Aïn Séfra (Atlas saharien, Algérie). Thèse Doctorat d'Etat. Université Pierre et Marie Curie, Paris (France), 320pp.

Hofmann, A.W., 1988. Chemical differentiation of the Earth: The relationship between mantle, continental-crust, and oceanic-crust. Earth and Planetary Science Letters, 90, 297-314.

Jourdan, F., Marzoli, A., Bertrand, H., Cirilli, S., Tanner, L., Kontak, D.J., McHone, G., Renne, P.R., Bellieni, G., 2009. 40Ar/39Ar ages of CAMP in North America: implications for the Triassic-Jurassic boundary and the 40K decay constant bias. Lithos, 110, 167-180.

Kazi-Tani, N., 1986. Evolution géodynamique de la bordure Nord-africaine: le domaine intraplaque nord-algérien. Approche mégaséquentielle. Thèse Doctorat d'Etat. Université de Pau (France), 784pp.

Knight, K.B., Nomade, S., Renne, P.R., Marzoli, A., Bertrand. H., Youbi, N., 2004. The Central Atlantic magmatic province at the Triassic-Jurassic boundary: paleomagnetic and 40Ar/39Ar evidence from Morocco for brief episodic volcanism. Earth and Planetary Science Letters, 228, 143-160.

Laville, E., Petit J.P., 1984. Role of synsedimentary strike-slip faults in the formation of Moroccan Triassic basins. Geology, 12, 424-427.

Laville, E., Piqué, A., 1991. La distension crustale atlantique et atlasique au Maroc au début du Mésozoïque: le rejeu des structures hercyniennes. Bulletin de la Société Géologique de France, 162(6), 1161-1171.

Le Bas, M.J., LeMaitre, R., Streckeisen, A., Zanettin, B., 1986. A chemical classification of volcanic rocks based on the total alkali silica diagram. Journal of Petrology, 27, 745-750.

Le Roy, P., Piqué, A., 2001. Triassic-Liassic Western Moroccan synrift basins in relation to the Central Atlantic Opening. Marine Geology, 172, 359-381.

Mahmoudi, A., Bertrand, H., 2007. Geochemical identification of the Central Atlantic magmatic province in folded domains, exemplified by the Moroccan Middle Atlas. Comptes Rendus Geoscience, 339, 545-552.

Marzoli, A., Renne, P.R., Piccirillo, E.M., Ernesto, M., Bellieni, G., De Min, A., 1999. Extensive 200 Million-Year-Old

Continental Flood Basalts of the Central Atlantic magmatic province. Science, 284, 616-618.

Marzoli, A., Bertrand, H., Knight, K.B., Cirilli, S., Buratti, N., Verati, C., Nomade, S., Renne, P.R., Youbi, N., Martini, R., Allenbach, K., Neuwerth, R., Rapaille, C., Zaninetti, L., Bellieni, G., 2004. Synchrony of the Central Atlantic magmatic province and the Triassic-Jurassic boundary climatic and biotic crisis. Geology, 32, 973-976.

Marzoli, A., Jourdan, F., Puffer, J.H., Cuppone, T., Tanner, L.H., Weems, R.E., Bertrand, H., Cirilli, S., Bellieni, G., De Min, A., 2011. Timing and duration of the Central Atlantic magmatic province in the Newark and Culpeper basins, eastern U.S.A. Lithos, 122, 175-188.

Mattauer, M., Tapponnier, P., Proust, F., 1977. Sur les mécanismes de formation des chaines intracontinentales: l'exemple des chaînes atlasiques du Maroc. Bulletin de la Société Géologique de France, 19, 521-526.

McHone, J.G., 2000. None plume magmatism and tectonics during the opening of the central Atlantic Ocean. Tectonophysics, 316, 287-296.

Meddah, A., Bertrand, H., Elmi, S., 2007. The Central Atlantic magmatic province in the Ksour basin (Saharan Atlas, Algeria). Compte Rendus Geoscience, 339, 24-30.

Meddah, A., 2010. La province magmatique de l'Atlantique central (CAMP) dans le bassin des Ksour (Atlas Saharien occidental, Algérie). Thèse Doctorat Es-Sciences. Algérie, Université d'Oran, 144pp.

Megard-Galli, J., Faure, J.L., 1988. Tectonique distensive et sédimentation au Ladinien supérieur Carnien dans la zone briançonnaise. Bulletin de la Société Géologique France, IV, 5(8), 705-715.

Mékahli, L., 1995. Hettangien Bajocien supérieur des Monts des Ksour: Biostratigraphie, sédimentologie, évolution paléogéographique et stratigraphique séquentielle. Thèse Doctorat d'Etat. Algérie, Université d'Oran, 358pp.

Merle, R., Marzoli, A., Reisberg, L., Bertrand, H., Nemchin, A., Chiaradia, M., Callegaro, S., Jourdan, F., Bellieni, G., Dan Kontak, D., Puffer, J., McHone, J.G., 2014. Sr, Nd, Pb and Os isotope systematics of CAMP tholeiites from Eastern North America (ENA): Evidence of a subduction-enriched mantle source. Journal of Petrology, 55, 133-180.

Nomade, S., Knight, K.B., Beutel, E., Renne, P.R., Verati, C., Féraud, G., Marzoli, A., Youbi, N., Bertrand, H., 2007. Chronology of the Central Atlantic magmatic province: Implications for the Central Atlantic rifting processes and the Triassic-Jurassic biotic crisis. Palaeogeography, Palaeoclimatology, Palaeoecology, 244, 326-344.

Piqué, A., Laville, E., 1995. L'Ouverture initiale de l'Atlantique central. Bulletin de la Société Géologique de France, 166(6), 725-738.

Piqué, A., Laville, E., 1996. The Central Atlantic Rifting: Reactivation of Paleozoic structures? Journal of Geodynamics, 21, 235-255.

Piqué, A., Ait Brahim, L., Aït Ouali, R., Amrhar, M., Charroud, M., Gourmelen, C., Laville, E., Rekhiss, F., Tricart, P., 1998. Evolution structurale des domaines atlasiques du Maghreb au Meso-Cenozoique: le rôle des structures héritées dans la déformation du domaine atlasique de l'Afrique du Nord. Bulletin de la Société Géologique de France, 169, 797-810.

Schoene, B., Guex, J., Bartolini, A., Schaltegger, U., Blackburn, T.J., 2010. Correlating the end-Triassic mass extinction and flood basalt volcanism at the 100 ka level. Geology, 38, 387-390.

Sun, S.S., McDonough, W.F., 1989. Chemical and isotopic systematics of oceanic basalts: implications for mantle composition and processes. In: Saunders, A.D., Norry, M.J. (eds.). Magmatism in the Ocean Basins. Geological Society of London Special Publication, 42, 313-345.

Tanner, L.H., Lucas, S.G., Chapman, M.G., 2004. Assessing the record and causes of Late Triassic extinctions. Earth Science Review, 65, 103-139.

Thirlwall, F.M., Upton, B.G.J., Jenkins, C., 1994. Interaction between continental lithosphere and Iceland plume-Sr-Nd-Pb isotope geochemistry of Tertiary basalts, NE Greenland. Journal of Petrology, 35, 839-879.

Verati, C., Bertrand, H., Féraud, G., 2005. The farthest record of the Central Atlantic magmatic province into West Africa craton: Precise 40Ar/39Ar dating and geochemistry of Taoudenni basin intrusives (northern Mali). Earth and Planetary Science Letters, 235, 391-407.

Winchester, J.A., Floyd, P.A., 1977. Geochemical discrimination of different magma series and their differentiation products using immobile elements. Chemical Geology, 20, 325-343.

Yelles-Chaouche, A.K., Aït Ouali, R., Bracene, R., Derder, M.E.M., Djellit, H., 2001. Chronologie de l'ouverture du bassin des Ksour (Atlas saharien, Algérie) au début du Mesozoïque. Bulletin de la Société Géologique de France, 172(3), 285-293.

Manuscript received February 2016;
revision accepted October 2016;
published Online January 2017.

APPENDIX I

TABLE I. Major (wt.%) and trace (ppm) element composition of the volcanic units (Saharan Atlas, Algeria). Site numbers correspond to the diapiric sites (Figs. 1D; 3)

	Lower unit												Intermediate unit				
Site	1	1	1	1	1	1	1	4	7	7	5	5	1	1	6	6	6
GPS	32°23'56.71"N 0°47'38.25"W		32°23'55.23"N 0°48'6.32"W		32°24'32.15"N 0°47'42.43"W		32°24'29.20"N 0°47'13.55"W	32°44'38.38"N 0°28'3.70"W	32°54'9.58"N 0°17'9.01"W		32°44'2.72"N 0°8'1.54"W		32°24'17.71"N 0°47'26.85"W	32°23'57.37"N 0°47'52.87"W	32°50'34.19"N 0°13'18.37"		
Sample	BGO	BG3	B1.1.03	B1.2.03	Dj.1.1	Tb1.03	B5	Tiout	AFZ1	AFZH4	AO 1.2	AOMSH1	B6	BGC3'	MZH1	MZH5	MZ0114
SiO_2	50.81	51.00	50.64	50.23	49.61	50.78	51.1	52.3	51.09	51.33	51.70	51.42	52.46	52.38	50.87	51.03	51.98
Al_2O_3	13.71	12.48	13.55	13.65	13.48	13.7	13.68	13.5	13.55	13.64	13.53	13.53	13.28	13.87	14.10	14.14	13.96
Fe_2O_{3t}	9.68	10.19	10.48	10.85	10.93	11.38	10.66	11	10.43	10.66	11.03	12.24	10.51	9.32	10.55	10.66	10.33
MgO	7.92	8.53	8.53	8.28	8.64	7.42	8.2	6.3	7.49	7.73	6.77	7.83	7.37	7.4	8.05	7.97	7.55
CaO	7.67	7.15	7.21	6.83	7.28	8.42	6.49	9.7	8.38	8.11	6.51	3.69	7.39	8.66	6.94	6.78	7.57
Na_2O	1.74	2.78	1.67	1.57	2.03	2.2	2.32	2.7	2.35	2.47	1.97	1.97	2.6	2.42	1.97	2.03	2.57
K_2O	3.91	2.65	3.76	4.65	3.28	2.4	2.99	1.3	2.56	2.51	3.95	3.41	2.61	2.44	3.30	3.38	2.51
TiO_2	1.4	1.34	1.38	1.38	1.44	1.58	1.4	1.5	1.36	1.37	1.51	1.42	1.4	1.29	1.29	1.22	1.37
P_2O_5	0.17	0.16	0.16	0.16	0.17	0.14	0.18	0.2	0.15	0.16	0.17	0.16	0.17	0.16	0.14	0.13	0.15
MnO	0.14	0.15	0.14	0.16	0.17	0.16	0.17	0.3	0.15	0.14	0.15	0.16	0.18	0.18	0.17	0.17	0.17
H_2O^+	2.4	2.96	2.77	2.79	2.84	2.01	3.18	1.27	1.93	2.05	2.16	4.31	2.24	1.97	2.79	2.83	2.35
H_2O^-	0.29	0.4	0.27	0.19	0.21	0.14	0.31	0.17	0.21	0.21	0.12	0.14	0.18	0.15	0.26	0.29	0.15
TOTAL	99.84	99.79	100.56	100.74	100.08	100.33	100.68	100.24	99.65	100.38	99.57	100.28	100.39	100.24	100.43	100.63	100.66
[Mg#]	0.62	0.62	0.62	0.60	0.61	0.56	0.60	0.53	0.59	0.59	0.55	0.56	0.58	0.61	0.60	0.60	0.59
Sc	32	32	30	35	29	33	30	32	27	26	31	31	29	33	34	36	34
V	270	232	265	266	267	288	271	274	250	255	275	265	252	254	307	303	253
Cr	315	453	307	305	298	274	285	269	297	288	337	356	258	278	126	110	271
Co	36	45	41	41	40	45	44	36	38	38	33	31	41	37	36	37	40
Ni	95	116	105	100	99	95	93	84	88	88	88	91	92	81	68	68	89
Y	23	19	24	25	29	23	25	26	25	25	25	25	21	22	25	24	22
Rb			61			62		33					49				50
Sr			142			154		227					155				148
Ba			1354			573		374					926				597
Zr			142			125		161					122				115
Hf			3.61			3.13		3.92					3.49				3.58
Nb			10.36			9.40		11.42					10.42				10.66
Th			3.24			2.77		3.59					3.34				3.24
U			0.70			0.61		0.83					0.75				0.68
Ta			1.01			1.02		1.31					0.92				0.88
La			18.95			15.71		15.75					11.63				11.53
Ce			38.16			33.92		35.73					26.66				26.64
Pr			4.57			4.16		4.55					3.41				3.45
Nd			19.26			17.73		19.59					14.82				14.74
Sm			4.59			4.17		4.83					3.70				3.64
Eu			1.74			1.41		1.51					1.12				1.09
Gd			5.13			4.65		5.14					3.99				3.98
Tb			0.70			0.64		0.74					0.57				0.56
Dy			4.63			4.27		4.83					3.91				3.88
Ho			0.92			0.84		0.94					0.78				0.76
Er			2.64			2.46		2.75					2.33				2.24
Yb			2.33			2.19		2.38					2.10				1.98
Lu			0.30			0.28		0.31					0.27				0.28

	Upper unit																
Site	5	5	8	3	3	3	3	3	3	9	9	9	9	9	10	10	10
GPS	32°44'7.92"N 0°9'3.83"W		33°1'49.91"N 0°4'13.41'E	32°42'58.67"N 0°42'41.99"W		32°42'56.22"N 0°42'39.88"W				33°7'58.06"N 0°14'49.61"W			33° 8'18.42"N 0°14'43.89"W		33°25'48.17"N 0°33'46.17"E		
Sample	AO B4.2	AOB9.1	CHL	FC1	FC2	ELHFC3	ELH1	ELH2	SF 03	ML1	ML3	ML1.5H	MLB6	ML3.2S	ELK0207	ELK0307	ELK0414
SiO_2	49.93	52.08	50.38	50.2	49.23	49.9	50.48	49.5	49.41	51.18	50.49	50.61	49.38	50.87	50.51	50.77	50.48
Al_2O_3	14.34	14.54	14.73	14.73	14.36	14.5	14.62	14.6	14.64	14.36	14.38	14.26	14.04	14.22	14.16	14.44	14.5
Fe_2O_{3t}	12.14	10.46	11.04	9.92	10.46	9.9	10.12	10.3	10.86	9.7	10.03	9.99	10.2	10.3	10.02	9.33	9.85
MgO	8.19	8.11	7.82	8.22	8.99	8.5	8.22	8.7	8.64	7.51	7.69	7.72	7.4	7.42	7.97	8.43	8.62
CaO	5.55	1.87	7.39	8.28	7.51	7.6	6.55	7.4	8.44	8.25	7.85	7.72	7.94	7.96	8.87	8.38	8.54
Na_2O	3.5	0.35	2.04	1.99	1.93	2.1	1.72	2.1	2.09	2.3	1.75	2.32	1.69	2.07	1.83	1.8	2.05
K_2O	2.2	7.16	2.85	2.47	2.21	2.6	3.47	2.6	2.09	2.38	3.27	2.48	3.16	2.28	2.77	3.15	2.12
TiO_2	1.11	1.17	1.13	1.1	1.07	1.1	1.15	1.2	1.16	1.14	1.12	1.12	1.1	1.1	1.08	1.02	1.11
P_2O_5	0.12	0.13	0.12	0.12	0.12	0.1	0.13	0.1	0.12	0.12	0.12	0.12	0.12	0.11	0.12	0.11	0.12
MnO	0.19	0.15	0.14	0.18	0.18	0.2	0.13	0.2	0.21	0.19	0.25	0.24	0.25	0.18	0.18	0.17	0.19
H_2O^+	2.77	3.63	2.63	2.64	3.4	3.03	3.09	3.21	2.93	2.07	2.4	2.78	3.88	2.95	2.29	2.51	2.83
H_2O^-	0.09	0.15	0.31	0.26	0.27	0.26	0.2	0.25	0.24	0.15	0.22	0.28	0.32	0.33	0.32	0.32	0.16
TOTAL	100.13	99.8	100.58	100.11	99.73	99.79	99.88	100.16	100.83	99.35	99.57	99.64	99.48	99.79	100.12	100.43	100.57
[Mg#]	0.57	0.60	0.58	0.62	0.63	0.63	0.62	0.62	0.61	0.63	0.60	0.60	0.59	0.59	0.61	0.64	0.63
Sc	34	38	34	36	31	35	36	41	32	31	32	32	31	33	29	32	33
V	284	308	257	284	273	292	287	297	297	257	282	248	283	286	256	249	267
Cr	212	162	149	172	138	128	148	103	137	154	143	134	147	151	148	149	152
Co	44	49	44	34	38	34	35	35	38	36	35	40	34	39	37	40	38
Ni	83	81	78	86	79	75	80	71	86	75	71	75	74	76	77	85	84
Y	20	20	23	24	21	22	22	23	23	22	22	20	22	21	19	20	21
Rb				74					61								65
Sr				186					198								178
Ba				1129					1016								906
Zr				97					100								95
Hf				2.54					2.67								2.62
Nb				5.19					5.78								5.97
Th				1.64					1.71								1.73
U				0.39					0.41								0.43
Ta				0.83					0.82								0.83
La				7.52					8.09								7.98
Ce				19.23					19.66								19.59
Pr				2.62					2.66								2.67
Nd				11.84					12.26								11.93
Sm				3.21					3.32								3.27
Eu				1.12					1.15								1.18
Gd				3.49					3.56								3.61
Tb				0.58					0.59								0.57
Dy				3.94					4.01								3.89
Ho				0.80					0.82								0.79
Er				2.38					2.43								2.38
Yb				2.18					2.26								2.12
Lu				0.28					0.29								0.29